



## Original Article

## Gallic acid protect against spinal cord ischemia-reperfusion injury in rat via activation of Nrf2/HO-1 signaling

Zhengqiang Liu <sup>a, b, d, 1</sup>, Huili Cai <sup>c, 1</sup>, Tianlun Wang <sup>e</sup>, Hamza bin Aleem <sup>a</sup>, Rui Liu <sup>f</sup>, Haidan Chen <sup>a, \*</sup><sup>a</sup> Department of Spinal Surgery, The First College of Clinical Medical Science, China Three Gorges University & Yichang Central People's Hospital, Yichang, Hubei, 443003, China<sup>b</sup> Department of Orthopaedics, Affiliated Hospital of Jiujiang University, Jiujiang, Jiangxi, 332000, China<sup>c</sup> Department of Hematology, The First College of Clinical Medical Science, China Three Gorges University & Yichang Central People's Hospital, Yichang, Hubei, 443003, China<sup>d</sup> Central Laboratory, The First College of Clinical Medical Science, China Three Gorges University, Yichang 443003, China<sup>e</sup> College of Medicine and Health Sciences, China Three Gorges University, Yichang 443003, China<sup>f</sup> Department of Cardiology, The First College of Clinical Medical Science, China Three Gorges University, Yichang, Hubei, 443002, China

## ARTICLE INFO

## Article history:

Received 19 January 2025

Received in revised form

22 March 2025

Accepted 29 March 2025

## Keywords:

Gallic acid

Spinal cord ischemia-reperfusion injury

Nrf2/HO-1 pathway

Neuronal apoptosis

Oxidative stress

## ABSTRACT

**Object:** This study explores Gallic acid's (GA) neuroprotective effects against spinal cord ischemia-reperfusion injury (SCII) and its underlying mechanisms.**Methods:** Spinal cord ischemia/reperfusion injury was induced in rats using the modified Zivin's method of clamping the abdominal aorta. The Basso-Beattie-Bresnahan scores, the inclined plane test, hematoxylin and eosin (HE) staining, and Nissl staining were used to measure locomotor activity and histological changes in the injured spinal cords. Proinflammatory factors (TNF- $\alpha$  and IL-1 $\beta$ ) were examined using an ELISA kit. Moreover, In vitro oxidative stress model was induced by tBHP used to assess the cell survival rate, reactive oxygen species (ROS) levels, Malondialdehyde (MDA) levels. RT-qPCR and Western blot was used to detect the expression levels of mRNA and proteins.**Results:** In vitro, GA inhibited tBHP-induced apoptosis in PC-12 cells, reduced ROS and MDA production, and abolished the expression of pro-apoptotic factors while enhancing the Nrf2/HO-1 signaling pathway. In vivo, GA treatment improved the behavioral and structural aspects of SCII in rats, inhibiting the production of proinflammatory factors, also reduced oxidative stress, and prevented neuronal apoptosis by enhancing the Nrf2/HO-1 signaling pathway.**Conclusions:** GA exhibits neuroprotective effects against SCII, involving antioxidant, anti-inflammatory, and anti-apoptotic activities through Nrf2/HO-1 signaling pathway.© 2025 The Author(s). Published by Elsevier BV on behalf of The Japanese Society for Regenerative Medicine. This is an open access article under the CC BY-NC-ND license (<http://creativecommons.org/licenses/by-nc-nd/4.0/>).

## 1. Introduction

Spinal cord ischemia-reperfusion injury (SCII) occurs when blood flow is restored after the removal of factors causing spinal cord ischemia, exacerbating spinal cord trauma [1]. SCII commonly

follows aortic aneurysm repair or spinal cord decompression procedures. This condition leads to neurological dysfunction, lower limb paralysis, and other unpredictable, catastrophic consequences, imposing a significant burden on patients and society [2]. Despite the proposal of substantial therapeutic interventions aimed at

\* Corresponding author. Spine surgery of Yichang Central People's Hospital, The First College of Clinical Medical Science, China Three Gorges University, Yichang, Hubei, 443002, China.

E-mail addresses: [liuzqzq@126.com](mailto:liuzqzq@126.com) (Z. Liu), [fujiancai.huili@sina.com](mailto:fujiancai.huili@sina.com) (H. Cai), [l792119250@qq.com](mailto:l792119250@qq.com) (T. Wang), [hamzaaleem@live.com](mailto:hamzaaleem@live.com) (H. Aleem), [2935059836@qq.com](mailto:2935059836@qq.com) (R. Liu), [chenhaidan1982@163.com](mailto:chenhaidan1982@163.com) (H. Chen).

Peer review under responsibility of the Japanese Society for Regenerative Medicine.

<sup>1</sup> Contributed equally.

mitigating neurological damage post-SCII, such as lumbar cerebrospinal fluid drainage, epidural hypothermia protocols, and intraoperative monitoring of somatosensory and motor-evoked potential, their overall effectiveness remains limited [3].

The various pathophysiological mechanisms implicated in SCII have undergone extensive evaluation, with one predominant perspective suggesting that neuronal demise is primarily induced through apoptosis [4,5]. The reperfusion process is characterized by an excessive production of Reactive Oxygen Species (ROS), which triggers neuronal apoptosis through protein degradation, lipid peroxidation, and DNA damage [6]. Oxidative stress activates microglial cells and astrocytes, leading to the release of an excess of pro-inflammatory mediators that can harm neighboring neurons. Moreover, it contributes to the disruption of the blood-spinal cord barrier (BSCB), spinal cord edema, and the influx of neutrophils following spinal cord ischemia [7]. Hence, addressing and alleviating oxidative stress, as well as the resulting inflammatory responses and apoptotic pathways, may present a novel approach to neuroprotection.

Recent research reveals that Nuclear Factor Erythroid 2-related Factor 2 (Nrf2) plays a pivotal role in signaling the antioxidant response element (ARE)-mediated regulation of gene expression [8]. Nrf2, a redox-sensitive transcription factor, binds to the ARE promoter under conditions of oxidative or electrophilic stress, thereby inducing a multitude of antioxidant and cytoprotective genes. These genes encompass superoxide dismutase (SOD), catalase, and heme oxygenase-1 (HO-1), which are involved in the management of oxidative stress, inflammatory responses, and apoptosis in various neurological disorders [9,10]. Thus, the pharmacological induction of the Nrf2 pathway may serve as a potent strategy for neuroprotection.

Plant-derived natural products have consistently demonstrated potent neuroprotective activities, signifying their potential relevance in treating neurological disorders. One such compound, Gallic acid (GA or 3,4,5-trihydroxy benzoic acid), is a naturally occurring phenolic molecule prevalent in various fruits and medicinal plants [11]. GA exhibits a range of beneficial properties including antioxidant, anti-inflammatory, and neuroprotective actions and transported across the blood-brain barrier [12,13]. Despite these attributes, its specific impact on SCII remains inadequately documented. Therefore, this study aims to elucidate the effects of GA on SCII and comprehend the mechanisms underlying these effects.

## 2. Materials and methods

### 2.1. Cell culture

The highly differentiated rat pheochromocytoma line PC-12 was procured from the Institute of Biochemistry and Cell Biology, SIBS, CAS (Shanghai, China). Cells were cultured in DMEM medium (HyClone, Logan, UT, United States) supplemented with 10 % fetal bovine serum (Hyclone) and 1 % penicillin-streptomycin (Beyotime, China) in a humidified incubator set to 37 °C with 95 % air and 5 % CO<sub>2</sub>.

### 2.2. Cell proliferation analysis through CCK-8 assay

Cell viability was evaluated using the CCK-8 assay on PC-12 cells, which were plated at a density of 5000 cells per well in 96-well plates. Subsequently, the cells were treated with *tert*-butyl hydroperoxide (tBHP, Sigma-Aldrich, St. Louis, MO) at concentrations ranging from 0 to 300 μM for 1 h, followed by exposure to varying concentrations of GA (0–3.2 μM) for 24 h. After treatment, the cells were washed with phosphate-buffered saline (PBS), and 10 μl of CCK-8 solution was added to each well. The plates were incubated at 37 °C for 1 h, and absorbance was measured at 450 nm using a microplate reader. Each experiment was performed in quintuplicate.

### 2.3. Determination of ROS production

Intracellular ROS levels were measured using the Reactive Oxygen Species Assay Kit (Beyotime, S0033, China) following the manufacturer's instructions. PC12 cells were washed with PBS and incubated with 5 μM DCFH-DA in phenol red-free DMEM medium for 30 min at 37 °C in the dark. After washing with serum-free medium, ROS-positive cells were visualized using a fluorescence microscope (Spectra MAX, Gemini EM, Molecular Devices, Sunnyvale, CA).

### 2.4. Animals

Fifty adult male Sprague-Dawley rats, weighing between 200 and 230 g, were obtained from the Model Animal Research Center, China Three Gorges University. All animals were housed in polypropylene cages under controlled conditions, including a room temperature of 22 ± 3 °C, a relative humidity of 50 ± 15 %, and a 12-h light/dark cycle. The rats had unrestricted access to standard rodent chow and water. None of the animals exhibited any neurological abnormalities prior to anesthesia and surgery. All procedures involving animals adhered to university policies and followed the NIH Guidelines for the Care and Use of Laboratory Animals. The study was approved by China Three Gorges University under Research Approval No. XJTULAC2018-454.

### 2.5. Drug treatment

All SD rats were randomly assigned to one of four groups: the sham group, the SCIRI group, and two GA treatment groups. The GA treatment groups were subdivided into a high-dose (100 mg/kg/day) group and a low-dose (50 mg/kg/day) group. The high-dose group comprised 8 rats, while each of the other three groups included 14 rats. Rats in the GA treatment groups were administered intraperitoneal injections of GA once daily for 7 days prior to the operation, while the control group received saline. Subsequently, SCII was performed in all groups except the Sham group. The sham group underwent exposure of the abdominal aorta without clamping. Post-surgery, animals in the GA treatment groups were promptly administered GA, while the control group received an equivalent volume of normal saline.

### 2.6. SCII model

Rats were anesthetized with 2 % isoflurane and positioned in a recumbent posture. Heparin (170 IU/kg) was administered subcutaneously 5 min before the procedure. The surgical area was disinfected with 75 % ethanol, and a 3 cm incision was made along the midline of the left rib cage. The left kidney and abdominal aorta were then identified. The abdominal aorta below the renal artery was occluded for 60 min using a 10 g aortic clamp, inducing spinal cord ischemic injury. The wounds were covered with saline-soaked gauze, and the arterial clamp was removed after 60 min. The abdominal cavity was closed after applying and spreading penicillin powder.

### 2.7. Behavioral tests

Functional deficits following injury were assessed as previously described [14,15]. Behavioral analyses were performed by trained investigators who were blind as to the experimental conditions. Hindlimb locomotor function was evaluated using the Basso-Beattie-Bresnahan (BBB) locomotion scale in an open-field test. The BBB scale is a 22-point system (scores 0–21) that systematically assesses the recovery of hindlimb function, from 0 (no observed hindlimb

movements) to 21 (normal ambulation). In the inclined plane test, rats were evaluated in two orientations (right side up or left side up) on the testing apparatus. The maximum angle at which a rat could maintain its position for 5 s without falling was recorded for each orientation and averaged to obtain a single score per animal.

2.8. Tissue preparation

Rats were anesthetized 24 h after reperfusion, except those used for behavioral scoring, and perfused via cardiac puncture first with saline and then with 4 % paraformaldehyde. The spinal cords (L2–L5) were dissected, removed, and fixed in 4 % paraformaldehyde overnight. The spinal cord tissue was dehydrated in 20 % and 30 % sucrose solutions before embedding in paraffin and sectioning into 10 μm thick serial coronal sections. For molecular analysis, rats were perfused with saline, and the L2–L5 spinal cord segments were isolated and stored at –80 °C until further use.

2.9. H&E staining

10 μm sections of paraffin-embedded tissue were cut, deparaffinized with xylene and graded ethanol, and then mounted on slides for hematoxylin and eosin (H&E) staining. An independent observer, blinded to the experimental conditions, captured images using an inverted fluorescence microscope (Nikon Eclipse T3-S, Tokyo, Japan).

2.10. Nissl staining

Nissl bodies, which are characteristic basophilic structures in neurons, were visualized using Nissl staining. Frozen spinal cord sections were sequentially immersed in distilled water, chloroform, 100 % ethanol, 95 % ethanol, and 75 % ethanol, each for 1 min. The sections were then stained with cresyl violet (FD Neuro Technologies, MD, USA) at 37 °C for 10 min. Following staining, sections were rinsed twice with distilled water and decolorized twice with 95 % ethanol. Dehydration was achieved using a graded series of ethanol (85 %, 80 %, and 75 %), after which the sections were air-dried. Finally, tissues were cleared with xylene and neutral gum, and mounted for examination under an optical microscope.

2.11. Malondialdehyde (MDA) concentration determination

Intracellular and spinal cord tissue levels of malondialdehyde (MDA) were quantified using an MDA assay kit (Beyotime, S0131, China) following the manufacturer's protocol. Briefly, treated cells and spinal cord tissues were lysed and centrifuged at 10,000×g for 10 min at 4 °C. MDA concentrations were determined by measuring absorbance at 532 nm using a spectrophotometer.

2.12. Reverse transcription real-time polymerase chain reaction (qRT-PCR)

Total RNA was extracted from L2–L5 spinal cord specimens and cells using TRIzol reagent (Invitrogen, USA). cDNA synthesis was performed with the HiScript III 1st Strand cDNA Synthesis Kit (Vazyme, R312, China). Quantitative real-time PCR was conducted with ChamQ Blue Universal SYBR qPCR Master Mix (Vazyme, Q312, China) on an ABI 7500 qRT-PCR instrument (Applied Biosystems). Primer sequences, synthesized by Genotech (Sangon Biotech, China), are listed in Table 1. Each sample was analyzed in triplicate, and relative gene expression was calculated using the 2<sup>–ΔΔCt</sup> method with β-actin as a reference.

**Table 1**  
Primer sequences used in qRT-PCR.

Target	Primer sequences (forward)	Primer sequences (reverse)
Bax	AAACTGGTGCTCAAGGCC	GGGTCCCGAAGTAGGAAAGG
Bcl-2	TGGAGAGCGTCAACAGGGAGATG	GGTGTGCAGATGCCGGTTCAG
Nrf2	TGTCAGCTACTCCCAGGTG	AGGGCAAGCGACTGAAATGT
HO-1	GGGTCAGGTGTCCAGGGAAGG	TGGGTTCTGCTTGTTCGCTCTATC
β-actin	GCTGTGCTATGTTGCCCTAGACTTC	GGAACCGCTCATTGCCGATAGTG

2.13. Western blotting

Protein was extracted from cells and tissues, and concentrations were determined using a BCA assay (Beyotime, China). Proteins were separated by SDS-polyacrylamide gel electrophoresis and transferred to a polyvinylidene fluoride (PVDF) membrane. The membrane was blocked with 5 % skim milk for 1 h at room temperature, then incubated overnight at 4 °C with primary antibodies. Subsequently, the membrane was incubated with horseradish peroxidase (HRP)-conjugated secondary antibodies for 2 h at room temperature. Protein bands were visualized using an ECL detection kit (Servicebio, China), and band intensities were quantified using ImageJ 6.0 software. Data are derived from at least three independent experiments.

2.14. Enzyme-Linked Immunosorbent assay (ELISA)

For ELISA, protein extraction followed the same procedure as for Western blotting. The levels of TNF-α and IL-1β were quantified using commercial ELISA kits (Servicebio, China) according to the manufacturer's instructions. Results are expressed as picograms per milligram (pg/mg) of protein.

2.15. Statistical analysis

Statistical analyses were performed using Prism 6.02 software (GraphPad Software, San Diego, CA, USA). Data are presented as mean ± standard error of the mean (SEM). Comparisons among groups were conducted using one-way analysis of variance (ANOVA) with Bonferroni's post hoc test for multiple comparisons. A p-value of <0.05 was considered statistically significant.

3. Results

3.1. Effects of tBHP or its combination with GA on PC-12 viability

To determine the toxicity effect of tBHP on PC-12 cells, cell viability was evaluated by using CCK8 assay. As shown in Fig. 1A, the cell viability of PC-12 dramatically decreased in a concentration-dependent manner after tBHP treatment (50–300 μM). In addition, tBHP treatment (75 μM) almost led to 40 % cell death, which was used for the subsequent experiments to evaluate the protective effect of GA.

To further explore the protective effect of GA on tBHP-induced PC-12 cell oxidative damage, the cells were treated with 75 μM of *tert*-butyl hydroperoxide (tBHP) for 1h, followed with GA (0.2–3.2 μM) treatment for 24 h. The results revealed that GA treatment significantly increased cell viability, compared to cells induced by tBHP alone. Pre-incubation with 0.2, 0.4, 0.8 and 1.6 μM of GA prevented cell death under oxidative stress, 0.8 μM GA works best in promoting healing of tBHP-induced cell injury, and thus we chose the 0.8 μM concentration for subsequent experiments. (Fig. 1B).

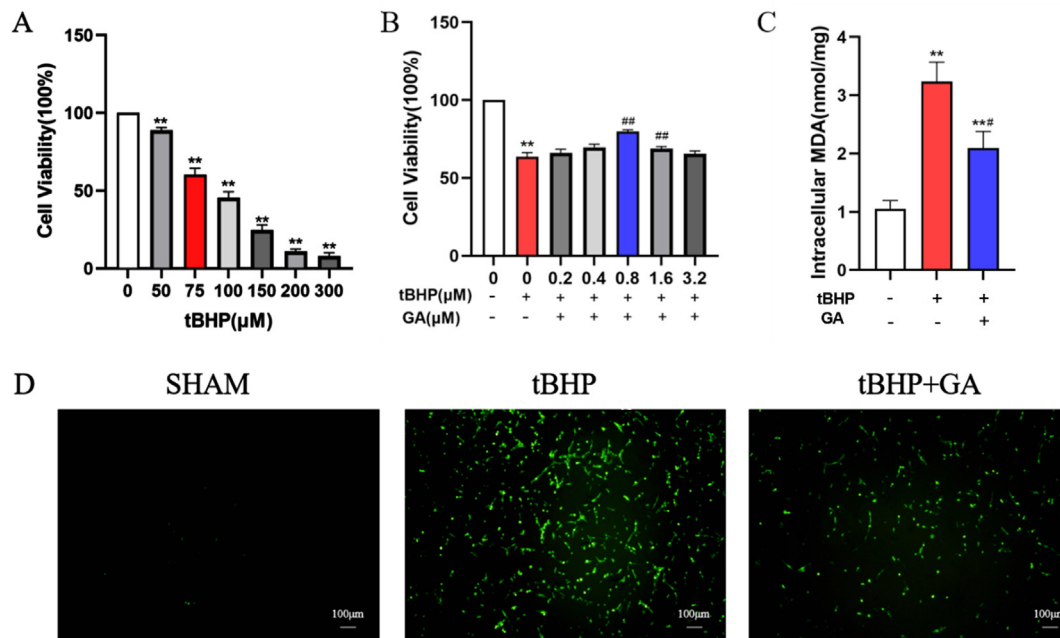


**Fig. 1.** GA protects PC-12 cells from tBHP-induced oxidative stress injury: (A) Viability of PC-12 cells treated with various concentrations of tBHP, as assessed by the CCK8 assay. (B) Protective effects of different concentrations of GA on tBHP-damaged PC-12 cells. (C) Impact of GA on the MDA level in tBHP-treated PC-12 cells. (D) Fluorescence images observed under an inverted fluorescence microscope, indicating GA decreased the level of reactive oxygen species (ROS) in tBHP-induced PC-12 cells. Data presented are the means  $\pm$  SD from Five independent experiments (\*\* $p < 0.01$ , versus SHAM group; # $p < 0.05$  or ## $p < 0.01$ , versus tBHP group).

### 3.2. GA prevented intracellular ROS generation and inhibited the release of MDA

To determine whether GA may attenuate tBHP-induced cell death through reducing oxidative stress, the levels of ROS and MDA were measured. As shown in Fig. 1C, Treatment of PC-12 cells with 75  $\mu$ M tBHP triggered a significant increase of MDA. However, treatment with GA significantly prevented the MDA release. tBHP treatment significantly upregulated mitochondrial ROS fluorescent signal in PC-12 cells compared to the control group, while treatment with GA significantly lowered mitochondrial ROS production (Fig. 1D).

### 3.3. Effects of GA on Nrf2/HO-1 pathways and apoptosis in tBHP-Induced PC-12 cells

To assess whether the cytoprotective effects of GA arise from its anti-oxidative and anti-apoptotic properties, we examined the mRNA transcript levels of the oxidative stress pathway Nrf2/HO-1, and the apoptotic marker Bax/Bcl2 in tBHP-treated PC-12 cells. As illustrated in Fig. 2, tBHP treatment resulted in notably reduced Nrf2 and Bcl2 expression, while significantly elevating Bax and HO-1 expression. Conversely, GA counteracted the tBHP-induced changes in apoptotic marker and Nrf2 mRNA levels, and further augmented HO-1 mRNA expression. Consequently, GA reduced oxidative stress and inhibited apoptosis under tBHP-induced oxidative damage by activating the Nrf2/HO-1 signaling pathway.

### 3.4. GA protected spinal cord tissue and improved functional recovery from SCII

To explore the therapeutic potential of GA on motor recovery post-SCII, we conducted BBB and inclined plane tests at 2h, 24h, 48h, and 72h post-injury. As depicted in Fig. 3, the SHAM group displayed severe neurological impairments following SCII

( $p < 0.01$ ). Nonetheless, GA significantly improved the BBB scores and maximal angles from 2h to 72h after injury ( $p < 0.05$  or  $p < 0.01$ ), indicating the enhancement of impaired neurological function. Moreover, no significant difference was found in BBB scores and the inclined plane test results between the 50 mg/kg and 100 mg/kg GA treatment groups post-injury ( $p > 0.05$ ).

Furthermore, HE staining results demonstrated well-maintained spinal cord tissues in the sham group, and neurons were morphologically normal with few vacuolar changes. In the SCII group, the number of normal neurons significantly decreased. Neurons were a great deal of vacuolization and slight bruising. In the GA (50 and 100 mg/kg) group, these pathological changes were markedly reduced compared with the SCII group, and the number of normal neurons was significantly greater than in the SCII group. NISSL staining results were approximately the same as HE staining, and GA significantly increased the number of Nissl-positive neurons compared with the SCII group. However, the neurons morphologically and content of Nissl bodies did not change much in 50 mg/kg compared with 100 mg/kg.

### 3.5. Determination of MDA content in spinal cord tissues

To examine the potential mechanism through which GA exerts its neuroprotective effects, we assessed the oxidative status in the spinal cord. Fig. 4c showcases a substantial increase in MDA content in the spinal cord following ischemia-reperfusion injury ( $p < 0.01$ ). On the contrary, ischemic tissues in the GA groups displayed a significant reduction in MDA levels, suggesting GA's ability to attenuate oxidative stress injury caused by SCII ( $p < 0.01$ ).

### 3.6. Determination of TNF- $\alpha$ and IL-1 $\beta$ content in spinal cord tissues

To assess the anti-inflammatory impact of GA on rats with spinal cord ischemia-reperfusion (SCII), we measured the pro-



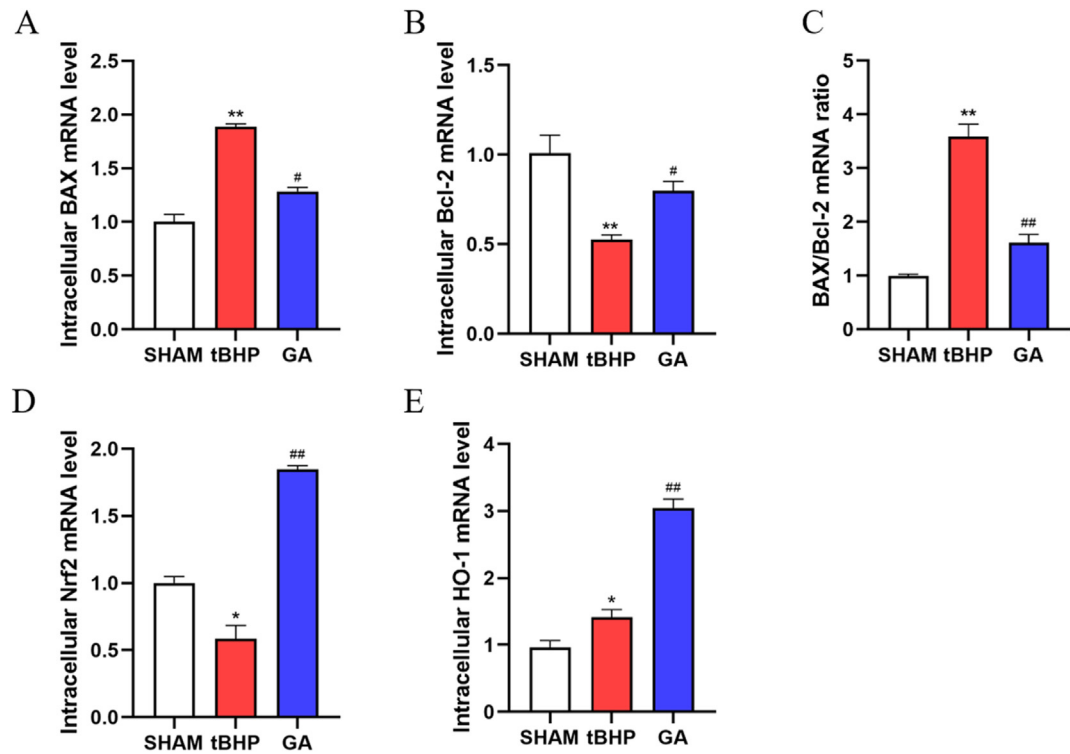


**Fig. 2.** Effect of GA on mRNA expression of apoptosis-regulating genes and the Nrf2/HO-1 signaling pathway in tBHP-treated PC-12 cells. (A) The impact of GA on BAX mRNA levels following tBHP injury. (B) The effect of GA on Bcl-2 mRNA levels after tBHP injury. (C) The effect of GA on the relative change of the BAX/Bcl-2 ratio after tBHP injury was analyzed. (D–E) The effects of GA on mRNA expression of the Nrf2/HO-1 signaling pathway following tBHP treatment. (\*\* $p < 0.01$ , versus SHAM group; # $p < 0.05$  or ## $p < 0.01$ , versus tBHP group).

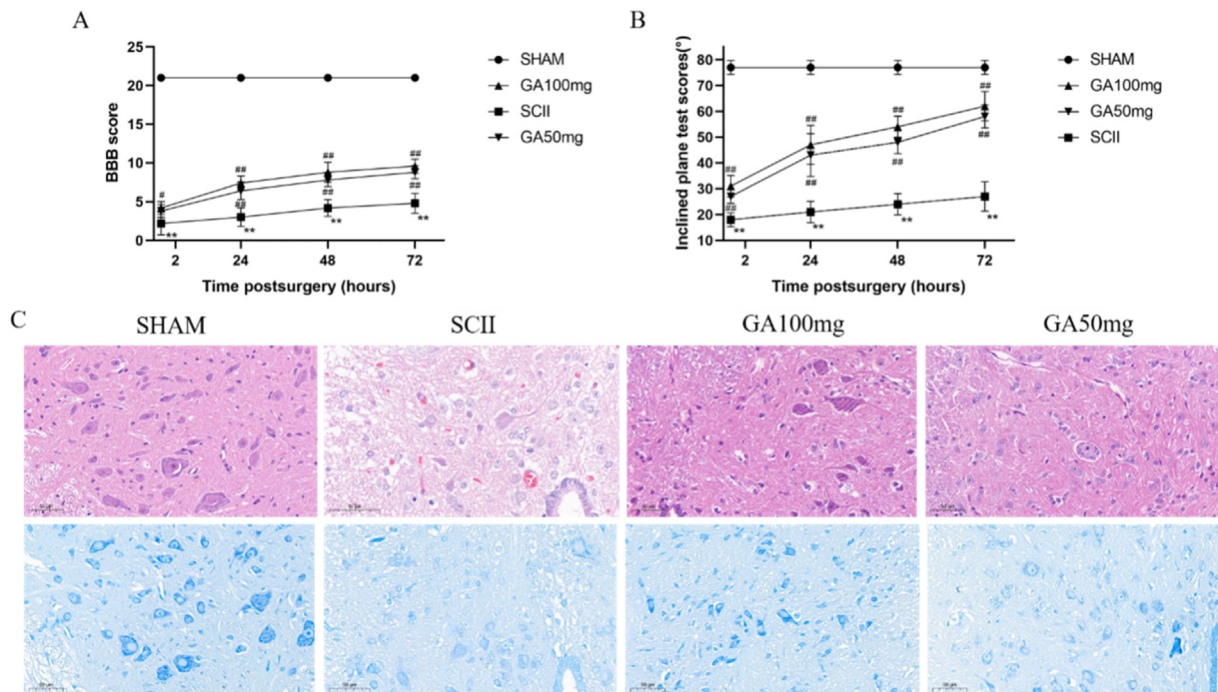


**Fig. 3.** GA improves motor function and spinal cord morphology in rats following SCI injury: (A) BBB scores were monitored daily for 72 h post-injury. The SHAM group consistently exhibited a score of 21, indicating no impairment, while the SCI group showed substantial functional deficits. In contrast, the GA-treated group demonstrated significant recovery in BBB scores. (B) During the slope experiment, the GA group displayed a considerable improvement in comparison to the SCI group at all time points. (C) The SCI group showed a significant reduction in the number of motor neurons and slight hemorrhage, which was attenuated by GA treatment. Similar findings were observed in Nissl staining. (\*\* $p < 0.01$ , versus SHAM group; # $p < 0.05$  or ## $p < 0.01$ , versus SCI group).

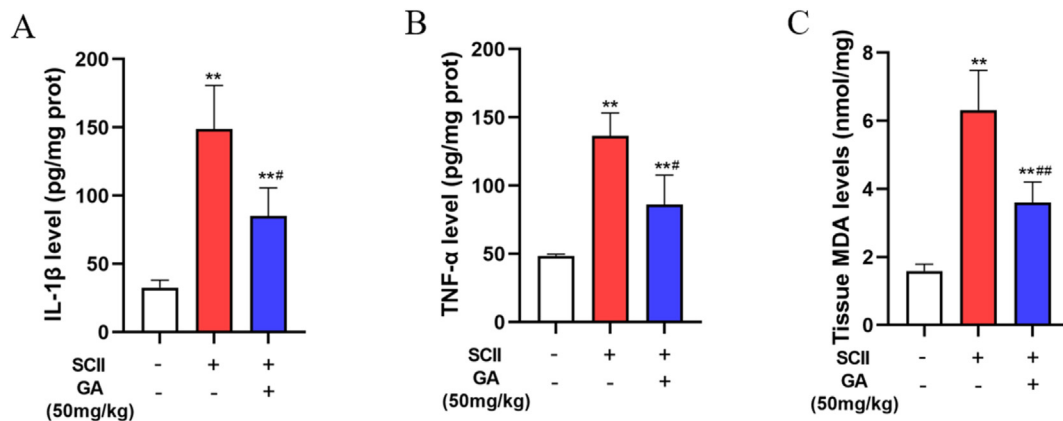


**Fig. 4.** The activities of tumor necrosis factor- $\alpha$  (TNF- $\alpha$ ) and interleukin-1 $\beta$  (IL-1 $\beta$ ), along with the levels of malondialdehyde (MDA), in rat spinal cord tissues (\*\* $p < 0.01$ , versus SHAM group; # $p < 0.05$  or ## $p < 0.01$ , versus SCII group,  $n = 4$ ).

inflammatory cytokines. We observed significantly higher levels of TNF- $\alpha$  and IL-1 $\beta$  in the spinal cord in the SCII group compared to the sham group ( $p < 0.01$ ). In contrast, the levels of TNF- $\alpha$  and IL-1 $\beta$  were significantly decreased in the animals that were treated with GA (Fig. 4,  $p < 0.05$ ).

### 3.7. GA normalized the expression of apoptosis-related mRNA and proteins in SCII rats

The effects of GA on apoptosis-related genes such as Bax and Bcl-2 were examined at mRNA and protein levels by RT-qPCR and Western blotting. Fig. 5A–D showed that the spinal cord of the SCII group expressed higher levels of Bax ( $P < 0.05$ ) but lower levels of Bcl-2 ( $P < 0.05$ ) compared with those of the Sham group. The administration of GA clearly decreased both the protein and mRNA expression of Bax, while concurrently increasing Bcl-2 protein and mRNA expression ( $P < 0.05$ ). And led to a significant reduction in the Bcl-2/Bax expression ratio ( $P < 0.05$ ).

### 3.8. GA exerted a neuroprotective effect by modulating the Nrf2/HO-1 pathways

RT-qPCR results revealed that mRNA levels of Nrf2 and HO-1 were significantly lower in the SCII groups than in the SHAM group ( $P < 0.01$ ) (Fig. 5A–E). GA enhanced the mRNA expressions of Nrf2 and HO-1 compared with the SCII group ( $P < 0.01$ ). Western blotting showed that the protein levels of Nrf2, HO-1 were significantly higher in the GA group than in the SHAM and SCII groups. ( $P < 0.05$ ) (Fig. 5F–M). These results demonstrated that the protective effects of GA on SCII oxidative stress and neurological function were dependent on Nrf2/HO-1 pathways.

## 4. Discussion

In this study, we confirmed for the first time that GA exerts a neuroprotective effect against SCII. Our study demonstrated that such neuroprotection by GA was most likely accomplished by activating the Nrf2/HO-1 pathway, which protected neurons by increasing the antioxidant activities and suppressing neuronal apoptosis by regulating the antioxidative injury and blocking apoptosis.

Oxidative stress is an important mechanism in spinal cord ischemia-reperfusion. In the early stage of reperfusion, massive ROS are produced for the appearance of abundant oxygen and

glucose. Then, the excessive ROS would further attack lipid and protein including antioxidant enzymes. The damage will be aggravated for the interruption of the antioxidant defense system [16]. Thus, in order to assess the neuroprotective potential of GA, an in vitro model of tBHP-induced oxidative damage was established using PC12 cells. Therefore, to evaluate the neuroprotective efficacy of GA, the researchers developed an in vitro tBHP-induced oxidative damage model using PC12 cells. The study found that GA provided protection against tBHP-induced oxidative stress and reduced the production of ROS and MDA. Furthermore, in vivo experiments revealed that GA preserved the neurological function of SCII rats and decreased the levels of MDA, TNF- $\alpha$ , and IL-1 $\beta$ .

Spinal cord ischemia/reperfusion induces the production and release of excessive free radicals and ROS, which induce mitochondrial membrane permeabilization, release cytochrome c to the cytoplasm, and activate caspase-9 and -3, subsequently initiating apoptosis [6,17]. Accumulating evidence indicates that apoptosis to be the main pattern of neuronal injury in patients suffering from secondary paralysis after spinal cord ischemia/reperfusion injury [5,6,18]. Bax (pro-apoptotic member) and Bcl-2 (anti-apoptotic member) belong to the Bcl-2 protein family and are a pair of antagonistic proteins and are key molecules in the process of cell apoptosis. Bcl-2 protein inhibits cell apoptosis, and Bax protein combines with Bcl-2 to form a complex, which promotes the degradation of Bcl-2 to relieve the inhibitory effect of Bcl-2 on cell apoptosis [19,20]. Additionally, whether apoptosis occurs is determined by the Bcl-2/Bax expression ratio, and a decrease in the Bcl-2/Bax ratio has been reported to be related to an increase in apoptosis [21].

Nrf2, a basic-leucine zipper transcription factor, is one of the important transcription factors in the endogenous defense system. The Nrf2-mediated signaling pathway can alleviate ischemia-reperfusion injury through antioxidative stress, antiapoptosis, anti-inflammation, and other ways; it has been used as a key target for the treatment of SCII [36]. Studies have shown that after the ischemia-reperfusion injury, oxygen free radicals can trigger Nrf2 phosphorylation and nuclear translocation, initiate the transcription of the downstream target gene HO-1, and induce the production of a variety of endogenous antioxidant enzymes, thereby reducing or eliminating the production of oxygen free radicals, resulting in redox balance in the body [37, 38]. A large number of studies confirmed that the Nrf2/HO-1 pathway plays an important role in antioxidant stress and apoptosis [36]. In the present study, we showed that GA treatment increased mRNA expression of Nrf2/

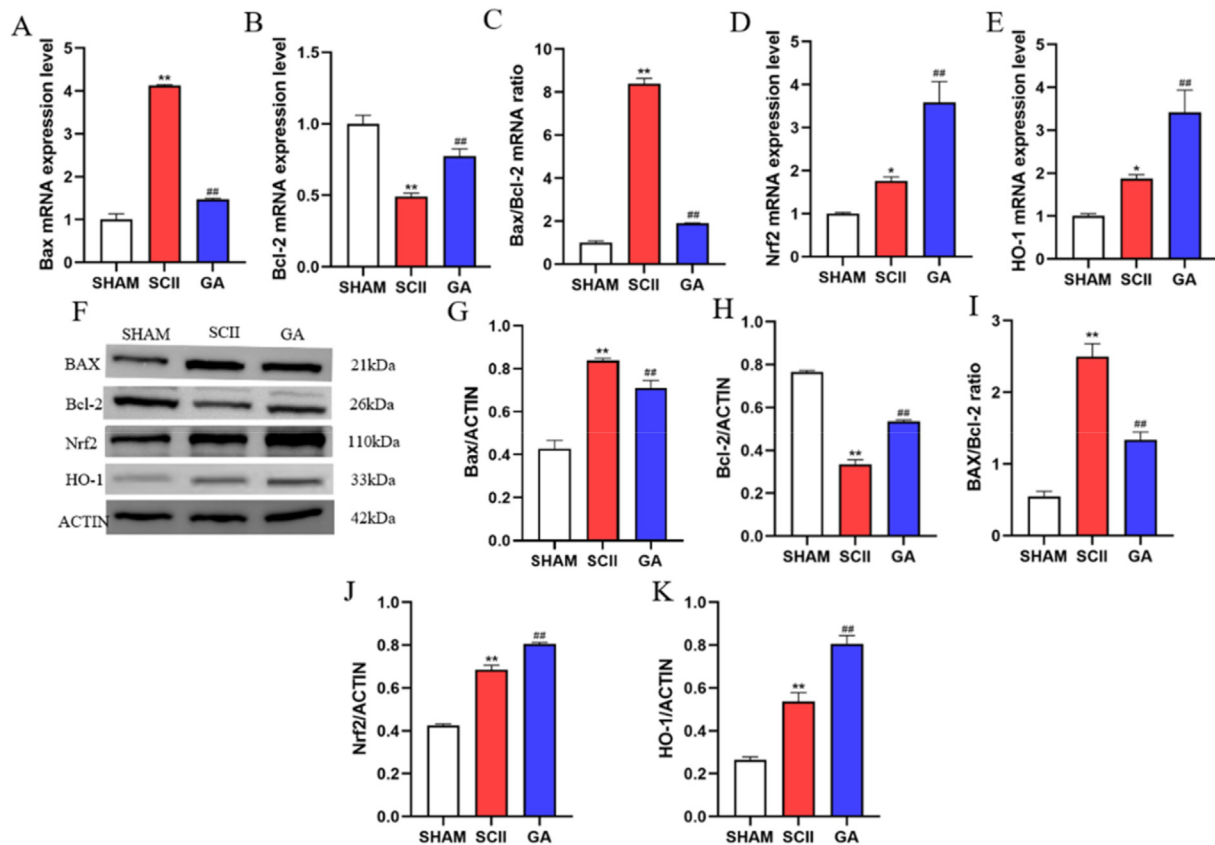


**Fig. 5.** The Effects of GA on Neuronal Apoptosis and the Nrf2/HO-1 Signaling Pathway Following SCII in Rats. (A–C) The Influence of GA on mRNA Levels Related to Apoptosis After SCII Injury in Rats. (D–E) The Influence of GA on mRNA Levels of the Nrf2/HO-1 Pathway After SCII Injury in Rats. (F–K) Western Blot Analysis of BAX, Bcl-2, Nrf2, and HO-1 Protein Expression After SCII Injury in Rats (\*\* $p < 0.01$ , versus SHAM group; # $p < 0.05$  or ## $p < 0.01$ , versus SCII group,  $n = 3$ ).

HO-1 in PC-12 cells. Moreover, Consistent with the results of the in vitro findings, we observed that Nrf2, HO-1 mRNA and protein expression levels increased after SCII. GA treatment significantly upregulated the levels of Nrf2 and HO-1, This suggests that methane may activate Nrf2/HO-1 pathways in both direct and indirect manner.

For the method of administration used in this study (50 mg/kg GA was administrated for 7 days ahead of SCII, i.p.). According to previous studies, 10 mg/kg–100 mg/kg GA exhibited the neuroprotective effect against cerebral ischemia/reperfusion injury and spinal cord injury. Park et al. showed that no statistically significant difference in the protective effect of GA (50 mg/kg or 100 mg/kg i.p.) in spinal cord injury of rats [12]. When we used different concentrations of GA (50 mg/kg or 100 mg/kg) to tested the efficacy treat SCII rats. Although the BBB scale and inclined plane test was slightly reduced in 100 mg/kg of GA-treated group as compared with 50 mg/kg of GA-treated group, the effect was not statistically different. Meanwhile, there was also no significant difference between the two groups of HE staining and Nissl staining. Thus, we used the 50 mg/kg of GA throughout the experiment in consideration of safety aspects. Mansouri et al., reported that GA administration at a dose of 200 mg/kg prevents memory deficit and oxidative stress than 100 mg/kg [22]. Yadav et al., reported that the administration of 50, 100, and 200 mg/kg GA reduces ketamine-induced psychosis by reducing oxidative stress and inflammation in a dose-dependent manner in global ischemia-induced rats [23]. These results suggest that high dosage of GA may have a better effect after SCI. However, the cytotoxicity of GA autoxidation

causing cell apoptosis has also been reported [24]. Thus, determining the effect of the dose of GA on cell death after SCII needs to be investigated in the future study.

GA could be a potential therapeutic drug in the treatment of spinal cord ischemia/reperfusion injury. However, spinal cord ischemic injury is an extremely complex process involving a variety of factors, and additional underlying mechanisms need to be explored.

## 5. Conclusion

In summary, our findings showed that the neuroprotective effect of GA after SCII is mediated, in part, by activation of Nrf2/HO-1 pathway, which result in improved recovery of locomotor function, reduced inflammation, apoptosis and oxidative stress in rat model of SCII. Our study suggests that GA may be a potentially useful therapeutic agent for traumatic SCII.

## Informed consent statement

Not applicable.

## Data availability

The data used to support the findings of the study are available from the corresponding authors upon reasonable request.

## Institutional review board statement

The study was approved by China Three Gorges University under Research Approval No. XJTULAC2018-454.

## Funding

This work was supported by the Natural Science Foundation of Hubei Province [grant numbers: 2016CFB600].

## Declaration of competing interest

The authors declare that the research was conducted in the absence of any commercial or financial relationships that could be construed as a potential conflict of interest.

## Acknowledgments

Not applicable.

## References

- [1] Rong Y, Fan J, Ji C, Wang Z, Ge X, Wang J, et al. Usp11 regulates autophagy-dependent ferroptosis after spinal cord ischemia-reperfusion injury by deubiquitinating beclin 1. *Cell Death Differ* 2022;29(6):1164–75. <https://doi.org/10.1038/s41418-021-00907-8>.
- [2] Chen FS, Tong XY, Fang B, Wang D, Li XQ, Zhang ZL. The roles of microRNAs in spinal cord ischemia-reperfusion injury. *Neural Regen Res* 2022;17(12):2593–9. <https://doi.org/10.4103/1673-5374.339471>.
- [3] Ling X, Lu J, Yang J, Qin H, Zhao X, Zhou P, et al. Non-coding RNAs: emerging therapeutic targets in spinal cord ischemia-reperfusion injury. *Front Neurol* 2021;12:680210. <https://doi.org/10.3389/fneur.2021.680210>.
- [4] Foley LS, Fullerton DA, Bennett DT, Freeman KA, Mares J, Bell MT, et al. Spinal cord ischemia-reperfusion injury induces erythropoietin receptor expression. *Ann Thorac Surg* 2015;100(1):41–6. <https://doi.org/10.1016/j.athoracsur.2015.01.027>.
- [5] Sun Z, Zhao T, Lv S, Gao Y, Masters J, Weng H. Dexmedetomidine attenuates spinal cord ischemia-reperfusion injury through both anti-inflammation and anti-apoptosis mechanisms in rabbits. *J Transl Med* 2018;16(1):209. <https://doi.org/10.1186/s12967-018-1583-7>.
- [6] Wang L, Yao Y, He R, Meng Y, Li N, Zhang D, et al. Methane ameliorates spinal cord ischemia-reperfusion injury in rats: antioxidant, anti-inflammatory and anti-apoptotic activity mediated by nrf2 activation. *Free Radic Biol Med* 2017;103:69–86. <https://doi.org/10.1016/j.freeradbiomed.2016.12.014>.
- [7] Han Y, Li X, Yang L, Zhang D, Li L, Dong X, et al. Ginsenoside rg1 attenuates cerebral ischemia-reperfusion injury due to inhibition of nox2-mediated calcium homeostasis dysregulation in mice. *J Ginseng Res* 2022;46(4):515–25. <https://doi.org/10.1016/j.jgr.2021.08.001>.
- [8] Li J, Wang T, Liu P, Yang F, Wang X, Zheng W, et al. Hesperetin ameliorates hepatic oxidative stress and inflammation via the pi3k/akt-nrf2-are pathway in oleic acid-induced hep2 cells and a rat model of high-fat diet-induced nafld. *Food Funct* 2021;12(9):3898–918. <https://doi.org/10.1039/d0fo02736g>.
- [9] Zhang Q, Liu J, Duan H, Li R, Peng W, Wu C. Activation of nrf2/ho-1 signaling: an important molecular mechanism of herbal medicine in the treatment of atherosclerosis via the protection of vascular endothelial cells from oxidative stress. *J Adv Res* 2021;34:43–63. <https://doi.org/10.1016/j.jare.2021.06.023>.
- [10] Zheng W, Liu B, Shi E. Perillaldehyde alleviates spinal cord ischemia-reperfusion injury via activating the nrf2 pathway. *J Surg Res* 2021;268:308–17. <https://doi.org/10.1016/j.jss.2021.06.055>.
- [11] Bhuiya MS, Rahaman MM, Islam T, Bappi MH, Sikder MI, Hossain KN, et al. Neurobiological effects of gallic acid: current perspectives. *Chin Med* 2023;18(1):27. <https://doi.org/10.1186/s13020-023-00735-7>.
- [12] Park CS, Lee JY, Choi HY, Lee K, Heo Y, Ju BG, et al. Gallic acid attenuates blood-spinal cord barrier disruption by inhibiting jmd3 expression and activation after spinal cord injury. *Neurobiol Dis* 2020;145:105077. <https://doi.org/10.1016/j.nbd.2020.105077>.
- [13] Yang YH, Wang Z, Zheng J, Wang R. Protective effects of gallic acid against spinal cord injury-induced oxidative stress. *Mol Med Rep* 2015;12(2):3017–24. <https://doi.org/10.3892/mmr.2015.3738>.
- [14] Basso DM, Beattie MS, Bresnahan JC. A sensitive and reliable locomotor rating scale for open field testing in rats. *J Neurotrauma* 1995;12(1):1–21. <https://doi.org/10.1089/neu.1995.12.1>.
- [15] Rivlin AS, Tator CH. Objective clinical assessment of motor function after experimental spinal cord injury in the rat. *J Neurosurg* 1977;47(4):577–81. <https://doi.org/10.3171/jns.1977.47.4.0577>.
- [16] Manzanero S, Santoro T, Arumugam TV. Neuronal oxidative stress in acute ischemic stroke: sources and contribution to cell injury. *Neurochem Int* 2013;62(5):712–8. <https://doi.org/10.1016/j.neuint.2012.11.009>.
- [17] Wu CC, Bratton SB. Regulation of the intrinsic apoptosis pathway by reactive oxygen species. *Antioxidants Redox Signal* 2013;19(6):546–58. <https://doi.org/10.1089/ars.2012.4905>.
- [18] Liu XZ, Sun X, Shen KP, Jin WJ, Fu ZY, Tao HR, et al. Aldehyde dehydrogenase 2 overexpression inhibits neuronal apoptosis after spinal cord ischemia/reperfusion injury. *Neural Regen Res* 2017;12(7):1166–71. <https://doi.org/10.4103/1673-5374.211198>.
- [19] Wang C, Zhang L, Ndong JC, Hettighouse A, Sun G, Chen C, et al. Progranulin deficiency exacerbates spinal cord injury by promoting neuroinflammation and cell apoptosis in mice. *J Neuroinflammation* 2019;16(1):238. <https://doi.org/10.1186/s12974-019-1630-1>.
- [20] Zhao R, Wu X, Bi XY, Yang H, Zhang Q. Baicalin attenuates blood-spinal cord barrier disruption and apoptosis through pi3k/akt signaling pathway after spinal cord injury. *Neural Regen Res* 2022;17(5):1080–7. <https://doi.org/10.4103/1673-5374.324857>.
- [21] Abdel-Wahab A, Hassanin K, Mahmoud AA, Abdel-Badea W, Abdel-Razik AH, Attia EZ, et al. Physiological roles of red carrot methanolic extract and vitamin E to abrogate cadmium-induced oxidative challenge and apoptosis in rat testes: involvement of the bax/bcl-2 ratio. *Antioxidants* 2021;10(11). <https://doi.org/10.3390/antiox10111653>.
- [22] Mansouri MT, Farbood Y, Sameri MJ, Sarkaki A, Naghizadeh B, Rafeirad M. Neuroprotective effects of oral gallic acid against oxidative stress induced by 6-hydroxydopamine in rats. *Food Chem* 2013;138(2–3):1028–33. <https://doi.org/10.1016/j.foodchem.2012.11.022>.
- [23] Yadav M, Jindal DK, Dhingra MS, Kumar A, Parle M, Dhingra S. Protective effect of gallic acid in experimental model of ketamine-induced psychosis: possible behaviour, biochemical, neurochemical and cellular alterations. *Inflammopharmacology* 2018;26(2):413–24. <https://doi.org/10.1007/s10787-017-0366-8>.
- [24] Chang YJ, Hsu SL, Liu YT, Lin YH, Lin MH, Huang SJ, et al. Gallic acid induces necroptosis via tnfr-alpha signaling pathway in activated hepatic stellate cells. *PLoS One* 2015;10(3):e0120713. <https://doi.org/10.1371/journal.pone.0120713>.